

The missing link: discerning true from false negatives when sampling species interaction networks

Michael D. Catchen^{1,2} Timothée Poisot^{3,2} Laura J. Pollock^{1,2} Andrew Gonzalez^{1,2}

¹ McGill University ² Québec Centre for Biodiversity Science ³ Université de Montréal

Correspondance to:

Michael D. Catchen — michael.catchen@mcgill.ca

Abstract: Ecosystems are composed of networks of interacting species. These interactions allow communities of species to persist through time through both neutral and adaptive processes. Despite their importance, a robust understanding of (and ability to predict and forecast) interactions among species remains elusive. This knowledge-gap is largely driven by a shortfall of data—although species occurrence data has rapidly increased in the last decade, species interaction data has not kept pace, largely due to the effort required to sample interactions. This means there are many interactions between species that occur in nature, but we do not know these interactions occur because we have never observed them. These so-called “false-negatives” bias data and hinder inference about the structure and dynamics of interaction networks. Here, we show the realized number of false-negatives in data can be quite high, even in thoroughly sampled systems, due to variation in abundances in a community. We provide a null model of occurrence detection to estimate the false-negative rate in a given dataset. We also show how to directly incorporate uncertainty due to observation error into model-based predictions of interactions between species. One hypothesis is interactions between “rare” species are themselves rare because these species are less likely to encounter one-another than species of higher relative abundance, and this can (in part) explain the common pattern of nestedness in bipartite interaction networks. However, we demonstrate that across several datasets of spatial/temporally replicated networks, there are positive associations between species co-occurrence and interactions, which suggests these interactions among “rare” species actually exist but simply are not observed. Finally, we assess how false negatives influence various models of network prediction, and recommend directly accounting for observation error in predictive models. We conclude by discussing how the understanding of false-negatives can inform how we design monitoring schemes for species interaction surveys.

Keywords:

species interactions

network ecology

sampling effort

spatial ecology

null models

1 Introduction

2 Species interactions drive many processes in evolution and ecology. A better understanding of species
3 interactions is an imperative to understand the evolution of life on Earth, to mitigate the impacts of
4 anthropogenic change on biodiversity (Makiola *et al.* 2020), and for predicting zoonotic spillover of
5 disease to prevent future pandemics (Becker *et al.* 2021). At the moment we lack sufficient data to meet
6 these challenges (Poisot *et al.* 2021), largely because species interactions are hard to sample (Jordano
7 2016). Over the past few decades biodiversity data has become increasingly available through remotely
8 collected data and adoption of open data practices (Kenall *et al.* 2014; Stephenson 2020). Still, interaction
9 data remains relatively scarce because sampling typically requires human observation. This induces a
10 constraint on the amount, spatial scale, and temporal frequency of resulting data that it is feasible to
11 collect by humans. Many crowdsourced methods for biodiversity data aggregation (e.g. GBIF, eBird) still
12 rely on automated identification of species, which does not easily generalize to interaction sampling.
13 There is interest in using remote methods for interaction sampling, which primarily detect co-occurrence
14 and derive properties like species avoidance from this data (Niedballa *et al.* 2019). However, co-occurrence
15 itself is not necessarily indicative of an interaction (Blanchet *et al.* 2020). This is an example of semantic
16 confusion around the word “interaction”—for example one might consider competition a type of species
17 interaction, even though it is marked by a lack of co-occurrence between species, unlike other types of
18 interactions, like predation or parasitism, which require both species to be together at the same place and
19 time. Here we consider interaction in the latter sense, where two species have fitness consequences on
20 one-another if (and only if) they are in the sample place at the same time. In addition, here we only
21 consider direct (not higher-order) interactions.

22 We cannot feasibly observe all (or even most) of the interactions that occur in an ecosystem. This means
23 we can be confident two species actually interact if we have a record of it (assuming they are correctly
24 identified), but not at all confident that a pair of species *do not* interact if we have *no record* of those
25 species observed together. In other words, it is difficult to distinguish *true-negatives* (two species never
26 interact) from *false-negatives* (two species interact sometimes, but we do not have a record of this
27 interaction). For a concrete example of a false-negative in a food web, see fig. 1. Because even the most
28 highly sampled systems will still contain false-negatives, there is increasing interest in combining
29 species-level data (e.g. traits, abundance, range, phylogenetic relatedness, etc.) to build models to predict

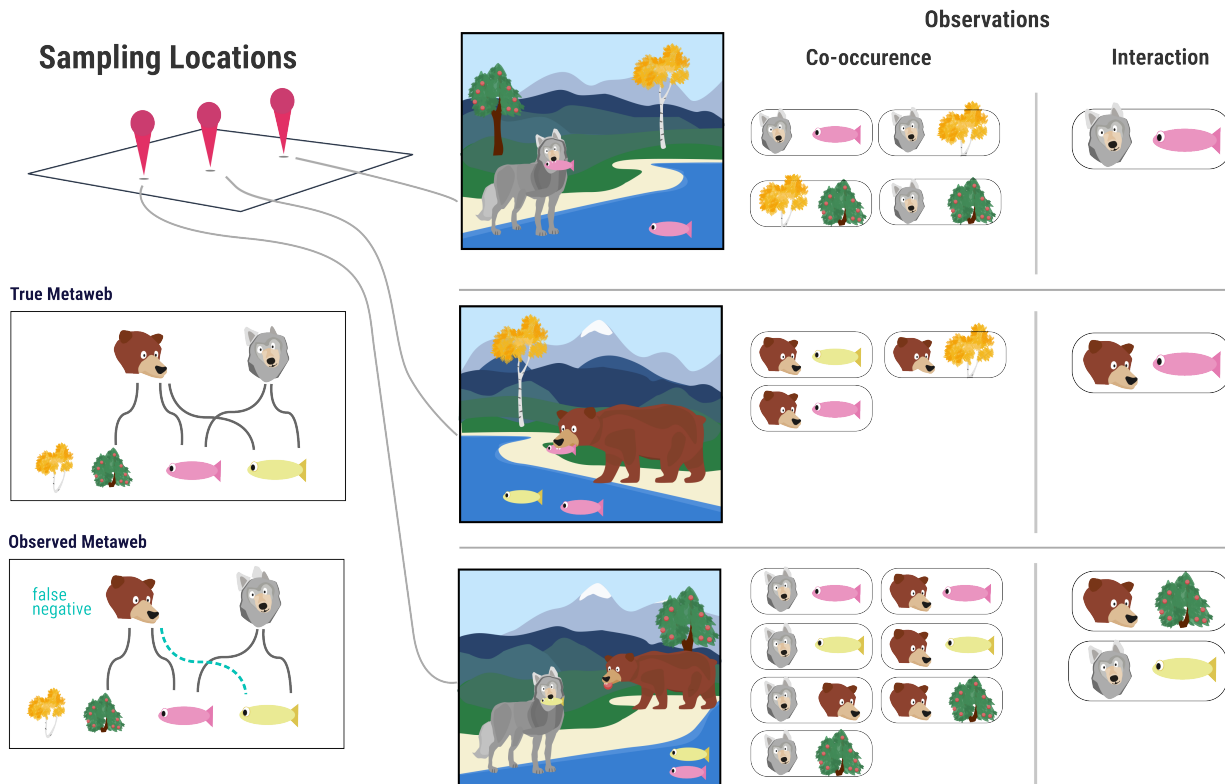


Figure 1: This conceptual example considers a sample of the trophic community of bears, wolves, salmon (pink fish), pike (yellow fish), berry trees, and aspen trees. The true metaweb (all realized interactions across the entire spatial extent) is shown on the left. In the center is what a hypothetical ecologist samples at each site. Notice that although bears are observed co-occurring with both salmon and pike, there was never a direct observation of bears eating pike, even though they actually do. Therefore, this interaction between bears and pike is a false-negative.

interactions between species we haven't observed together before (Strydom *et al.* 2021). However, the noise of false-negatives could impact the efficacy of our predictive models and have practical consequences for answering questions about interactions (de Aguiar *et al.* 2019). This data constraint is amplified as the interaction data we have is geographically biased toward the usual suspects (Poisot *et al.* 2021). We therefore need a statistical approach to assessing these biases in the observation process and their consequences for our understanding of interaction networks.

The importance of *sampling effort* and its impact on resulting ecological data has produced a rich body of literature. The recorded number of species in a dataset or sample depends on the total number of observations (Walther *et al.* 1995; Willott 2001), as do estimates of population abundance (Griffiths 1998). This relationship between sampling effort, spatial coverage, and species detectability has motivated more

40 quantitatively robust approaches to account for error in sampling data in many contexts: to determine if a
41 given species is extinct (Boakes *et al.* 2015), to determine sampling design (Moore & McCarthy 2016), and
42 to measure species richness across large scales (Carlson *et al.* 2020). In the context of interactions, an
43 initial concern was the compounding effects of limited sampling effort combined with the amalgamation
44 of data (across both study sites, time of year, and taxonomic scales) could lead any empirical set of
45 observations to inadequately reflect the reality of how species interact (Paine 1988) or the structure of the
46 network as a whole (Martinez *et al.* 1999; McLeod *et al.* 2021). Martinez *et al.* (1999) showed that in a
47 plant-endophyte trophic network, network connectance is robust to sampling effort, but this was done in
48 the context of a system for which observation of 62,000 total interactions derived from 164,000 plant-stems
49 was feasible. In some systems (e.g. megafauna food-webs) this many observations is either impractical or
50 infeasible due to the absolute abundance of the species in question.

51 The intrinsic properties of ecological communities create several challenges for sampling: first, species are
52 not observed with equal probability—we are much more likely to observe a species of high abundance
53 than one of very low abundance (Poisot *et al.* 2015). Canard *et al.* (2012) presents a null model of food-web
54 structure where species encounter one-another in proportion to each species' relative-abundance. This
55 assumes that there are no associations in species co-occurrence due to an interaction (perhaps because
56 this interaction is “important” for both species; Cazelles *et al.* (2016)), but in this paper we later show
57 increasing strength of these associations leads to increasing probability of false-negatives in interaction
58 data, and that these positive associations are common in existing network data. Second, observed
59 co-occurrence is often equated with meaningful interaction strength, but this is not necessarily the case
60 (Blanchet *et al.* 2020)—a true “non-interaction” would require that neither of two species, regardless of
61 whether they co-occur, ever exhibit any meaningful effect on the fitness of the other. So, although
62 co-occurrence is not directly indicative of an interaction, it is a precondition for an interaction.

63 Here, we illustrate how our confidence that a pair of species never interacts highly depends on sampling
64 effort. We demonstrate how the realized false-negative-rate of interactions is related to the relative
65 abundance of the species pool, and introduce a method to produce a null estimate of the false-negative-rate
66 given total sampling effort (the total count of all interactions seen among all species-pairs) and a method
67 for including uncertainty into model predictions of interaction probabilities to account for observation
68 error. We then confront these models with data, by showing that positive associations in co-occurrence
69 data can increase the realized number of false-negatives and by showing these positive associations are

70 rampant in network datasets. We conclude by recommending that the simulation of sampling effort and
71 species occurrence can and should be used to help design surveys of species interaction diversity (Moore &
72 McCarthy 2016), and by advocating use of null models like those presented here as a tool for both guiding
73 design of surveys of species interactions and for including detection error into predictive models.

74 **Accounting for false-negatives in species interactions**

75 In this section, we demonstrate how differences in species' relative-abundance can lead to many
76 false-negatives in interaction data. We also introduce a method for producing a null estimate of the
77 false-negative-rate in datasets via simulation. Because the true false-negative-rate is latent, we can never
78 actually be sure how many false-negatives are in our data. However, here we outline an approach to deal
79 with this fact—first by using simulation to estimate the false-negative-rate for a dataset of a fixed size
80 using neutral models of observation. We then illustrate how to incorporate uncertainty directly into
81 predictions of species interactions to account for observation error based on null estimates of both the
82 false-positive rate (as an *a priori* estimate of species misidentification probability) and false-negative rate
83 (as generated via the method we introduce).

84 **How many observations of a non-interaction do we need to be confident it's a true** 85 **negative?**

86 We start with a naive model of interaction detection: we assume that every interacting pair of species is
87 incorrectly observed as not-interacting with an independent and fixed probability, which we denote p_{fn}
88 and subsequently refer to as the False-Negative-Rate (FNR). If we observe the same species not-interacting
89 N times, then the probability of a true-negative (denoted p_{tn}) is given by $p_{tn} = 1 - (p_{fn})^N$. This relation
90 (the cumulative-distribution-function of geometric distribution, a special case of the negative-binomial
91 distribution) is shown in fig. 2(a) for varying values of p_{fn} and illustrates a fundamental link between our
92 ability to reliably say an interaction doesn't exist— p_{tn} —and the number of times N we have observed a
93 given species. In addition, note that there is no non-zero p_{fn} for which we can ever *prove* that an
94 interaction does not exist—no matter how many observations of non-interactions N we have, $p_{tn} < 1$.

95 From fig. 2(a) it is clear that the more often we see two species co-occurring, but *not interacting*, the more
96 likely the interaction is a true-negative. This has several practical consequences: first it means negatives

97 taken outside the overlap of the range of each species aren't informative because co-occurrence was not
 98 possible, and therefore neither was an interaction. In the next section we demonstrate that the
 99 distribution of abundance in ecosystems can lead to very high realized values of FNR (p_{fn}) simply as an
 100 artifact of sampling effort. Second, we can use this relation to compute the expected number of total
 101 observations needed to obtain a “goal” number of observations of a particular pair of species (fig. 2(b)). As
 102 an example, if we hypothesize that A and B do not interact, and we want to see species A and B both
 103 co-occurring and *not interacting* 10 times to be confident this is a true negative, then we need an expected
 104 1000 observations of all species if the relative abundances of A and B are both 0.1.

105 **False-negatives as a product of relative abundance**

106 We now show that the realized FNR changes drastically with sampling effort due to the intrinsic variation
 107 of the abundance of individuals of each species within a community. We do this by simulating the process
 108 of observation of species interactions, applied both to 243 empirical food webs from the Mangal database
 109 (Banville *et al.* 2021) and random food-webs generated using the niche model, a simple generative model
 110 of food-web structure that accounts for allometric scaling (Williams & Martinez 2000). Our neutral model
 111 of observation assumes each observed species is drawn in proportion to each species' abundance at that
 112 place and time. The abundance distribution of a community can be reasonably-well described by a
 113 log-normal distribution (Volkov *et al.* 2003). In addition to the log-normal distribution, we also tested the
 114 case where the abundance distribution is derived from power-law scaling $Z^{(\log(T_i)-1)}$ where T_i is the
 115 trophic level of species i and Z is a scaling coefficient (Savage *et al.* 2004), which yields the same
 116 qualitative behavior. The practical consequence of abundance distributions spanning many orders of
 117 magnitude is that observing two “rare” species interacting requires two low probability events: observing
 118 two rare species *at the same time*.

119 To simulate the process of observation, for an ecological network M with S species, we sample relative
 120 abundances for each species from a standard-log-normal distribution. For each true interaction in the
 121 adjacency matrix M (i.e. $M_{ij} = 1$) we estimate the probability of observing both species i and j at a given
 122 place and time by simulating n observations of all individuals of any species, where the species of the
 123 individual observed at the $\{1, 2, \dots, n\}$ -th observation is drawn from the generated categorical distribution
 124 of abundances. For each pair of species (i, j) , if both i and j are observed within the n -observations, the
 125 interaction is tallied as a true positive if $M_{ij} = 1$. If only one of i or j are observed—but not both—in these



Figure 2: **(a)** The probability that an observed interaction is a true negative (y-axis) given how many times it has been sampled as a non-interaction (x-axis). Each color reflects a different value of p_{fn} , the false-negative-rate (FNR)—this is effectively the cumulative distribution function (cdf) of the geometric distribution. **(b)** The expected number of total observations needed (colors) to observe 10 co-occurrences between a species with relative abundance $P(A)$ (x-axis) and a second species with relative abundance $P(Y)$. **(c)**: false-negative-rate (y-axis) as a function of total sampling effort (x-axis) and network size, computed using the method described above. For 500 independent draws from the niche model (Williams & Martinez (2000)) at varying levels of species richness (colors) with connectance drawn according to the flexible-links model (MacDonald *et al.* (2020)) as described in the main text. For each draw from the niche model, 200 sets of 1500 observations are simulated, for which the mean false-negative-rate at each observation-step is computed. Means denoted with points, with 1 in the first shade and 2 in the second. **(d)**: Same as **(c)**, except using empirical food webs from Mangal database, where richness. The outlier on **(d)** is a 714 species food-web.

126 n observations, but $M_{ij} = 1$, this is counted as a false-negative, and a true-negative otherwise. For each
 127 pair of species (i, j) , if both i and j are observed within the n -observations, the interaction is tallied as a
 128 true positive if $M_{ij} = 1$. If only one of i or j are observed—but not both—in these n observations, but
 129 $M_{ij} = 1$, this is counted as a false-negative, and a true-negative otherwise ($M_{ij} = 0$). This process is
 130 illustrated conceptually in fig. 3(a).

131 In fig. 2(c) we see this model of observation applied to niche model networks across varying levels of
 132 species richness, and in fig. 2(d) the observation model applied to Mangal food webs. For all niche model
 133 simulations in this manuscript, for a given number of species S the number of interactions is drawn from
 134 the flexible-links model fit to Mangal data (MacDonald *et al.* 2020), effectively drawing the number of
 135 interactions L for a random niche model food-web as

$$L \sim \text{BetaBinomial}(S^2 - S + 1, \mu\phi, 1 - \mu\phi)$$

136 where the maximum *a posteriori* (MAP) estimate of (μ, ϕ) applied to Mangal data from (MacDonald *et al.*
 137 2020) is $(\mu = 0.086, \phi = 24.3)$. All simulations were done with 500 independent replicates of unique niche
 138 model networks per unique number of total interactions observed n . All analyses presented here are done
 139 in Julia v1.8 (Bezanson *et al.* 2015) using both EcologicalNetworks.jl v0.5 and Mangal.jl v0.4 (Banville *et*
 140 *al.* 2021) and are hosted on Github (**link removed for double-blind review**). Note that the empirical
 141 data, for the reasons described above, very likely already contains many false-negatives, we'll revisit this
 142 issue in the final section.

143 From fig. 2(c) it is evident that the number of species considered in a study is inseparable from the
 144 false-negative-rate in that study, and this effect should be taken into account when designing samples of
 145 ecological networks in the future. We see a similar qualitative pattern in empirical networks (fig. 2(d))
 146 where the FNR drops off quickly as a function of observation effort, mediated by total richness. The
 147 practical consequence of the bottom row of fig. 2 when conducting an analysis is whether there are
 148 enough total number of observed interactions (the x-axis) for the threshold FNR we deem acceptable (the
 149 y-axis) is feasible. This raises two points: first, empirical data on interactions are subject to the practical
 150 limitations of funding and human-work hours, and therefore existing data tend to fall on the order of
 151 hundreds or thousands observations of individuals per site. Clear aggregation of data on sampling effort
 152 has proven difficult to find and a meta-analysis of network data and sampling effort seems both pertinent

and necessary, in addition to the effects of aggregation of interactions across taxonomic scales (Gauzens *et al.* 2013; Giacomuzzo & Jordán 2021). This inherent limitation on in-situ sampling means we should optimize where we sample across space so that for a given number of samples, we obtain the maximum information possible. Second, what is meant by “acceptable” FNR? This raises the question: does a shifting FNR lead to rapid transitions in our ability inference and predictions about the structure and dynamics of networks, or does it produce a roughly linear decay in model efficacy? We explore this in the final section. We conclude this section by advocating for the use of neutral models similar to above to generate expectations about the number of false-negatives in a dataset of a given size. This could prove fruitful both for designing surveys of interactions but also because we may want to incorporate models of imperfect detection error into predictive interactions models, as Joseph (2020) does for species occurrence modeling. Additionally, we emphasize that one must consider the context for sampling—is the goal to detect a particular species (as in fig. 2(c)), or to get a representative sample of interactions across the species pool? These arguments are well-considered when sampling individual species (Willott 2001), but have not yet been adopted for designing samples of communities.

Including observation error in interaction predictions

Here we show how to incorporate uncertainty into model predictions of interaction probability to account for imperfect observation (both false-negatives and false-positives). Models for interaction prediction typically yield a probability of interaction between each pair of species, p_{ij} . When these are considered with uncertainty, it is usually model-uncertainty, e.g. the variance in the interaction probability prediction across several cross-validation folds, where the data is split into training and test sets several times. The method we introduce adjusts the value of a model’s predictions to produce a distribution of interaction probabilities corrected by a given false-negative-rate p_{fn} and false-positive-rate p_{fp} (outlined in figure fig. 3). First we describe how to sample from this distribution of adjusted interaction probabilities via simulation, and show that this distribution can be well-approximated analytically.

To get an estimate of each interaction probability that accounts for observation error, we resample the output prediction from an arbitrary model for each interaction p_{ij} by simulating a set of several ‘particles.’ Each particle is a realization of an interaction *actually occurring* assuming p_{ij} is a correct estimate of the probability of an interaction being *observed*. Each particle starts as being drawn as true or false according

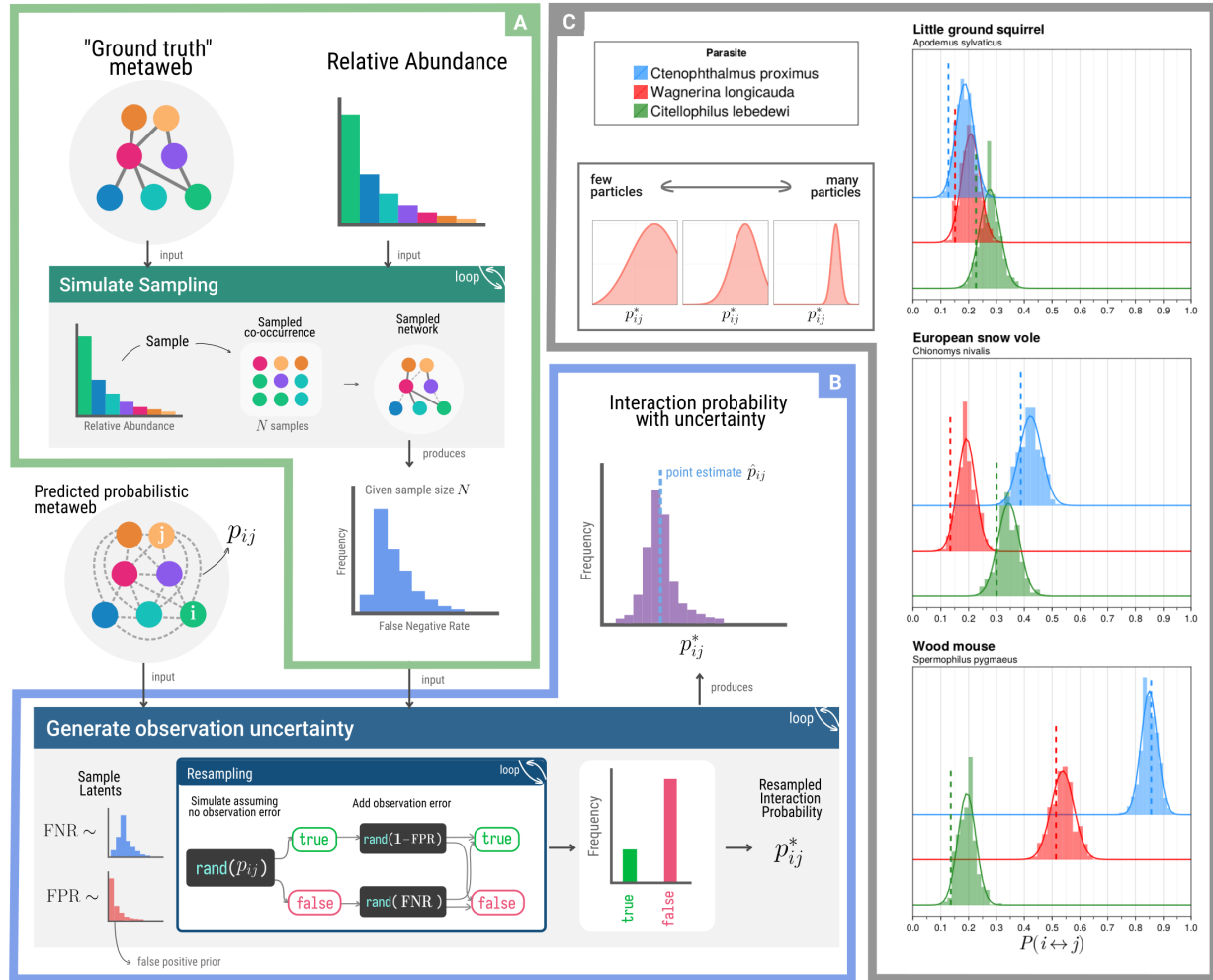


Figure 3: (a) The process for estimating the false-negative-rate (FNR) for an interaction dataset consisting of N total observed interactions. (b) The method for resampling interaction probability based on estimates of false-negative and false-positive rates. (c) The method for interaction probability resampling applied to three mammals and three parasites from the Hadfield *et al.* (2014) dataset. The original probability p_{ij} is indicated with a vertical dashed line. The histogram is simulated from the resampling process, and the line indicates the gaussian approximation to this distribution. Both resampling simulations and the gaussian approximation is applied with $n_p = 150$

181 to p_{ij} , and then adjusting this by the rate of observation error given by p_{fp} and p_{fn} to yield a single
 182 boolean outcome for each particle (“Resampling” within fig. 3(b)). Across of many particles, the resulting
 183 frequency of ‘true’ outcomes is a single resample of the probability p_{ij}^* that the interaction actually
 184 occurred, not just that it was observed. Across several samples each of several particles, this forms a
 185 distribution of probabilities which are adjusted by the true and false-negative-rates.

186 There is also an analytic way to approximate this distribution using the normal approximation to binomial.
 187 As a reminder, as the total number of samples N from a binomial distribution for n trials with success
 188 probability p from approaches infinity, the sum of total successes across all samples approaches a normal
 189 distribution with mean np and variance $np(1 - p)$. For notation, here we refer to a normal distribution
 190 with mean μ and standard-deviation σ as $\mathcal{N}(\mu, \sigma)$. We can use this to correct the estimate p_{ij} based on the
 191 expected false-negative-rate p_{fn} and false-positive rate p_{fp} to obtain the limiting distribution as the
 192 number of resamples approaches infinity for the resampled p_{ij}^* for a given number of particles n_p . We do
 193 this by first adjusting for the rates of observation error to get the mean resampled probability, $\mathbb{E}[p_{ij}^*]$, as

$$\mathbb{E}[p_{ij}^*] = p_{ij}(1 - p_{fp}) + (1 - p_{ij})p_{fn}$$

194 This yields the normal approximation

$$\sum_{i=1}^{n_p} p_{ij}^* \sim \mathcal{N}\left(n_p \cdot \mathbb{E}[p_{ij}^*], \sqrt{n_p \mathbb{E}[p_{ij}^*](1 - \mathbb{E}[p_{ij}^*])}\right)$$

195 which then can be converted back to a distribution of frequency of successes to yield the final
 196 approximation

$$p_{ij}^* \sim \mathcal{N}\left(\mathbb{E}[p_{ij}^*], \sqrt{\frac{\mathbb{E}[p_{ij}^*](1 - \mathbb{E}[p_{ij}^*])}{n_p}}\right) \quad (1)$$

197 We can then further truncate this distribution to remain on the interval $(0, 1)$, as the output is a
 198 probability, although in practice often the probability mass outside $(0, 1)$ is extremely low except for p_{ij}
 199 values very close to 0 or 1. As an example case study, we use a boosted-regression-tree to predict
 200 interactions in a host-parasite network (Hadfield *et al.* 2014) (with features derived in the same manner as
 201 Strydom *et al.* (2021) derives features on this data) to produce a set of interaction predictions. We then

202 applied this method to a set of a few resampled interaction probabilities between mammals and parasite
203 species shown in figure fig. 3(c).

204 Why is this useful? For one, this analytic method avoids the extra computation required by simulating
205 samples from this distribution directly. Further, it enables the extension of the natural analogue between
206 n_p (the number of particles) and the number of observations of co-occurrence for a given pair of
207 species—the fewer the particles, the higher the variance of the resulting approximation. The normal
208 approximation is undefined for 0 particles (i.e. 0 observations co-occurrence), although as n_p approaches 0
209 the approximated normal (once truncated) approaches the uniform distribution on the interval (0, 1), the
210 maximum entropy distribution where we have no information about the possibility of an interaction.

211 This also has implications for what we mean by ‘uncertainty’ in interaction predictions. A model’s
212 prediction can be ‘uncertain’ in two different ways: (1) the model’s predictions may have high variance, or
213 (2) the model’s predictions may be centered around a probability of interaction of 0.5, where we are the
214 most unsure about whether this interaction exists. Improving the incorporation of different forms of
215 uncertainty in probabilistic interaction predictions seems a necessary next step toward understanding
216 what pairs of species we know the least about, in order to prioritize sampling to provide the most new
217 information possible.

218 **Positive associations in co-occurrence increase the false-negative-rate**

219 The model above doesn’t consider the possibility that there are positive or negative associations which shift
220 the probability of species cooccurrence away from what is expected based on their relative abundances due
221 to their interaction (Cazelles *et al.* 2016). However, here we demonstrate that the probability of having a
222 false-negative can be higher if there is some positive association in the occurrence of species A and B . If
223 we denote the probability that we observe the co-occurrence of two species A and B as $P(AB)$ and if there
224 is no association between the marginal probabilities of observing A and observing B , denoted $P(A)$ and
225 $P(B)$ respectively, then the probability of observing their co-occurrence is the product of the marginal
226 probabilities for each species, $P(AB) = P(A)P(B)$. In the other case where there is some positive strength
227 of association between observing both A and B because this interaction is “important” for each species,
228 then the probability of observation both A and B , $P(AB)$, is greater than $P(A)P(B)$ as $P(A)$ and $P(B)$ are
229 not independent and instead are positively correlated, i.e. $P(AB) > P(A)P(B)$. In this case, the probability

of observing a single false-negative in our naive model from fig. 2(a) is $p_{fn} = 1 - P(AB)$, which due to the above inequality implies $p_{fn} > 1 - P(A)P(B)$. This indicates an increasingly greater probability of a false negative as the strength of association gets stronger, $P(AB) \rightarrow P(AB) \gg P(A)P(B)$. However, this still does not consider variation in species abundance in space and time (Poisot *et al.* 2015). If positive or negative associations between species structure variation in the distribution of $P(AB)$ across space/time, then the spatial/temporal biases induced by data collection would further impact the realized false-negative-rate, as the probability of false negative would not be constant for each pair of species across sites.

To test for these positive associations in data we scoured Mangal for datasets with many spatial or temporal replicates of the same system, which led to the resulting seven datasets set in figure fig. 4. For each dataset, we compute the marginal probability $P(A)$ of occurrence of each species A across all networks in the dataset. For each pair of interacting species A and B , we then compute and compare the probability of co-occurrence if each species occurs independently, $P(A)P(B)$, to the empirical joint probability of co-occurrence, $P(AB)$. Following our analysis above, if $P(AB)$ is greater than $P(A)P(B)$, then we expect our neutral estimates of the FNR above to underestimate the realized FNR. In fig. 4, we see the difference between $P(AB)$ and $P(A)P(B)$ for the seven suitable datasets with enough spatio-temporal replicates and a shared taxonomic backbone (meaning all individual networks use common species identifiers) found on Mangal to perform this analysis. Further details about each dataset are reported in tbl. 1.

In each of these datasets, the joint probability of co-occurrence $P(AB)$ is decisively greater than our expectation if species co-occur in proportion to their relative abundance $P(A)P(B)$. This suggests that there may not be as many “neutrally forbidden links” (Canard *et al.* 2012) as we might think, and that the reason we do not have records of interactions between rare species is probably due to observation error. This has serious ramifications for the widely observed property of nestedness seen in bipartite networks (Bascompte & Jordano 2007)—perhaps the reason we have lots of observations between generalists is because they are more abundant, and this is particularly relevant as we have strong evidence that generalism drives abundance (Song *et al.* 2022a), not vice-versa.

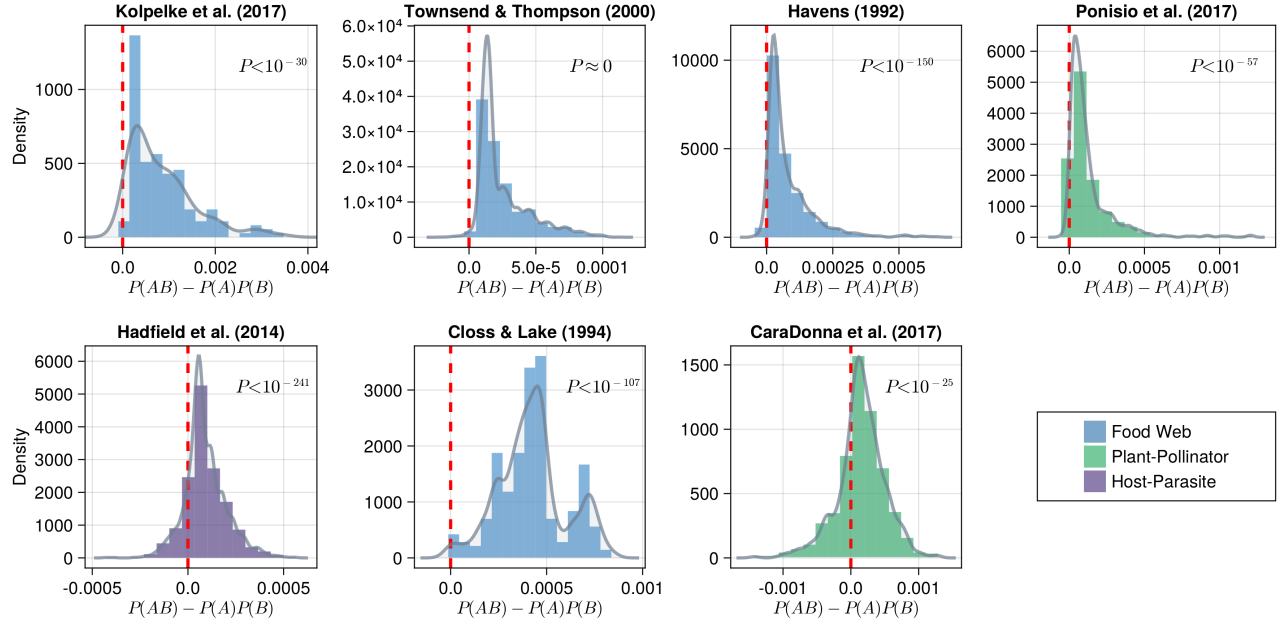


Figure 4: The difference between joint-probability of co-occurrence ($P(AB)$) and expected probability of co-occurrence under independence ($P(A)P(B)$) for interacting species for each dataset. The red-dashed line indicates 0 (no association). Each histogram represents a density, meaning the area of the entire curve sums to 1. The continuous density estimate (computed using local smoothing) is shown in grey. The p-value on each plot is the result of a one-sided t-test comparing the mean of each distribution to 0.

Table 1: The datasets used in the above analysis (Fig 2). The table reports the type of each dataset, the total number of networks in each dataset (N), the total species richness in each dataset (S), the connectance of each metaweb (all interactions across the entire spatial-temporal extent) (C), the mean species richness across each local network \bar{S} , the mean connectance of each local network \bar{C} , the mean β -diversity among overlapping species across all pairs of network species ($\bar{\beta}_{OS}$), and the mean β -diversity among all species in the metaweb ($\bar{\beta}_{WN}$). Both metrics are computed using KGL β -diversity (Koleff *et al.* 2003)

Network	Type	N	S	C	\bar{S}	\bar{C}	$\bar{\beta}_{OS}$	$\bar{\beta}_{WN}$
Kopelke <i>et al.</i> (2017)	Food Web	100	98	0.037	7.87	0.142	1.383	1.972
Thompson & Townsend (2000)	Food Web	18	566	0.014	80.67	0.049	1.617	1.594
Havens (1992)	Food Web	50	188	0.065	33.58	0.099	1.468	1.881
Ponisio <i>et al.</i> (2017)	Pollinator	100	226	0.079	23.0	0.056	1.436	1.870
Hadfield <i>et al.</i> (2014)	Host-Parasite	51	327	0.085	32.71	0.337	1.477	1.952
Closs & Lake (1994)	Food Web	12	61	0.14	29.09	0.080	1.736	1.864
CaraDonna <i>et al.</i> (2017)	Pollinator	86	122	0.18	21.42	0.312	1.527	1.907

The impact of false-negatives on network properties and prediction

Here, we assess the effect of false-negatives on our ability to make predictions about interactions, as well as their effect on network structure. The prevalence of false-negatives in data is the catalyst for interaction prediction in the first place, and as a result methods have been proposed to counteract this bias (Stock *et al.* 2017; Poisot *et al.* 2022). However, it is feasible that the FNR in a given dataset is so high that it could induce too much noise for an interaction prediction model to detect the signal of possible interaction between species.

To test this we use the dataset from Hadfield *et al.* (2014) that describes host-parasite interaction networks sampled across 51 sites, and the same method as Strydom *et al.* (2021) to extract latent features for each species in this dataset based on applying PCA to the co-occurrence matrix. We then predict a metaweb (equivalent to predicting true or false for an interaction between each species pair, effectively a binary classification problem) from these species-level features using four candidate models for binary classification—three often used machine-learning (ML) methods (Boosted Regression Tree (BRT), Random Forest (RF), Decision Tree (DT)), and one naive model from classic statistics (Logistic Regression (LR)). Each of the ML models are bootstrap aggregated (or bagged) with 100 replicates each. We partition the data into 80-20 training-test splits, and then seed the training data with false negatives at varying rates, but crucially do *nothing* to the test data. We fit all of these models using MLJ.jl, a high-level Julia framework for a wide-variety of ML models (Blaom *et al.* 2020). We evaluate the efficacy of these models using two common measures of binary classifier performance: the area under the receiver-operator curve (ROC-AUC) and the area under the precision-recall curve (PR-AUC), for more details see Poisot (2022). Here, PR-AUC is slightly more relevant as it is a better indicator of prediction of false-negatives. The results of these simulations are shown in fig. 5(a & b).

One interesting result seen in fig. 5(a & b) is that the ROC-AUC value does not approach random in the same way the PR-AUC curve does as we increase the added FNR. The reason for this is that ROC-AUC is fundamentally not as useful a metric in assessing predictive capacity as PR-AUC. As we keep adding more false-negatives, the network eventually becomes a zeros matrix, and these models can still learn to predict “no-interaction” for all possible species pairs, which does far better than random guessing (ROC-AUC = 0.5) in terms of the false positive rate (one of the components of ROC-AUC). This highlights a more broad issue of label class imbalance, meaning there are far more non-interactions than interactions in data. A



Figure 5: **(a)** The area-under the receiver-operator curve (ROC-AUC) and **(b)** The area-under the precision-recall curve (PR-AUC; right) for each different predictive model (colors/shapes) across a spectrum of the proportion of added false-negatives (x-axis). **(c)** The mean trophic-level of all species in a network generated with the niche model across different species richnesses (colors). For each value of the FNR, the mean trophic level was computed across 50 replicates. The shaded region for each line is one standard-deviation across those replicates.

284 full treatment of the importance of class-balance is outside the scope of this paper, but is explored in-depth
285 in Poisot (2022). Further we see, if anything, gradual decline in the performance of the model until we
286 reach very high FNR levels (i.e. $p_{fn} > 0.7$). This is consistent with other recent work (Gupta *et al.* 2023),
287 although it must be considered that the empirical data on which these models are trained already are
288 almost certain to already contain false-negatives.

289 Although these ML models are surprisingly performant at link prediction given their simplicity, there
290 have been several major developments in applying deep-learning methods to many tasks in network
291 inference and prediction—namely graph-representation learning (GRL, Khoshraftar & An (2022)) and
292 graph convolutional networks (Zhang *et al.* 2019). At this time, these advances can not yet be applied to
293 ecological networks because they require far more data than we currently have. We already have lots of
294 features that could be used as inputs into these models (i.e. species level data about occurrence, genomes,
295 abundance, etc.), but our network datasets barely get into the hundreds of local networks sampled across
296 space and time (tbl. 1). Once we start to get into the thousands, these models will become more useful, but
297 this can only be done with systematic monitoring of interactions. This again highlights the need to
298 optimize our sampling effort to maximize the amount of information contained in our data given the
299 expense of sampling interactions.

300 We also consider how the FNR affects network properties. In fig. 5(c) we see the mean trophic level across
301 networks simulated using the niche model (as above), across a spectrum of FNR values. In addition to the
302 clear dependence on richness, we see that mean trophic level, despite varying widely between niche model
303 simulations, tends to be relatively robust to false-negatives and does not deviate widely from the true value
304 until very large FNRs. This is not entirely unsurprising. Removing links randomly from a food-web is
305 effectively the inverse problem of the emergence of a giant component (more than half of the nodes are in
306 a connected network) in random graphs (see Li *et al.* (2021) for a thorough review). The primary
307 difference being that we are removing edges, not adding them, and thus we are witnessing the dissolution
308 of a giant component, rather than the emergence of one. Further applications of percolation theory (Li *et al.*
309 *al.* 2021) to the topology of sampled ecological networks could improve our understanding of how
310 false-negatives impact the inferences about the structure and dynamics on these networks.

311 Discussion

312 Species interactions enable the persistence and functioning of ecosystems, but our understanding of
313 interactions is limited due to the intrinsic difficulty of sampling them. Here we have provided a null
314 model for the expected number of false-negatives in an interaction dataset. We demonstrated that we
315 expect many false-negatives in species interaction datasets purely due to the intrinsic variation of
316 abundances within a community. We also, for the first time to our knowledge, measured the strength of
317 association between co-occurrence and interactions (Cazelles *et al.* 2016) across many empirical systems,
318 and found that these positive associations are both very common, and showed algebraically that they
319 increase the realized FNR. We have also shown that false-negatives could further impact our ability to
320 both predict interactions and infer properties of the networks, which highlights the need for further
321 research into methods for correcting this bias in existing data.

322 A better understanding of how false-negatives impact species interaction data is a practical
323 necessity—both for inference of network structure and dynamics, but also for prediction of interactions by
324 using species level information. False-negatives could pose a problem for many forms of inference in
325 network ecology. For example, inferring the dynamic stability of a network could be prone to error if the
326 observed network is not sampled “enough.” What exactly “enough” means is then specific to the
327 application, and should be assessed via methods like those here when designing samples. Further,
328 predictions about network rewiring (Thompson & Gonzalez 2017) due to range shifts in response to
329 climate change could be error-prone without accounting for interactions that have not been observed but
330 that still may become climatically infeasible. As is evident from fig. 2(a), we can never guarantee there are
331 no false-negatives in data. In recent years, there has been interest toward explicitly accounting for
332 false-negatives in models (Stock *et al.* 2017; Young *et al.* 2021), and a predictive approach to
333 networks—rather than expecting our samples to fully capture all interactions (Strydom *et al.* 2021). As a
334 result, better models for predicting interactions are needed for interaction networks. This includes
335 explicitly accounting for observation error (Johnson & Larremore 2021)—certain classes of models have
336 been used to reflect hidden states which account for detection error in occupancy modeling (Joseph 2020),
337 and could be integrated in the predictive models of interactions in the future.

338 This work has several practical consequences for the design of surveys for species’ interactions.

339 Simulating the process of observation could be a powerful tool for estimating the sampling effort required

by a study that takes relative abundance into account, and provides a null baseline for expected FNR. It is necessary to take the size of the species pool into account when deciding how many total samples is sufficient for an “acceptable” FNR (fig. 2(c & d)). Further the spatial and temporal turnover of interactions means any approach to sampling prioritization must be spatiotemporal. We demonstrated earlier that observed negatives outside of the range of both species aren’t informative, and therefore using species distribution models could aid in this spatial prioritization of sampling sites.

We also should address the impact of false-negatives on the inference of process and causality in community ecology. We demonstrated that in model food webs, false-negatives do not impact the measure of total trophic levels until very high FNR (figure fig. 5(c)), although we cannot generalize this further to other properties. This has immediate practical concern for how we design what taxa to sample—does it matter if the sampled network is fully connected? It has been shown that the stability of subnetworks can be used to infer the stability of the metaweb paper beyond a threshold of samples (Song *et al.* 2022b). But does this extend to other network properties? And how can we be sure we are at the threshold at which we can be confident our sample characterizes the whole system? We suggest that modeling observation error as we have done here can address these questions and aid in the design of samples of species interactions. To try to survey to avoid all false-negatives is a fool’s errand. Species ranges overlap to form mosaics, which themselves are often changing in time. Communities and networks don’t end in space, and the interactions that connect species on the ‘periphery’ of a given network to species outside the spatial extent of a given sample will inevitably appear as false-negatives in practical samples. The goal should instead be to sample a system enough to have a statistically robust estimate of the current state and empirical change over time of an ecological community at a given spatial extent and temporal resolution, and to determine what the sampling effort required should be prior to sampling.

References

- Banville, F., Vissault, S. & Poisot, T. (2021). Mangal.jl and EcologicalNetworks.jl: Two complementary packages for analyzing ecological networks in Julia. *Journal of Open Source Software*, 6, 2721.
- Bascompte, J. & Jordano, P. (2007). Plant-Animal Mutualistic Networks: The Architecture of Biodiversity. *Annual Review of Ecology, Evolution, and Systematics*, 38, 567–593.
- Becker, D.J., Albery, G.F., Sjödin, A.R., Poisot, T., Bergner, L.M., Dallas, T.A., *et al.* (2021). Optimizing

368 predictive models to prioritize viral discovery in zoonotic reservoirs.

369 Bezanson, J., Edelman, A., Karpinski, S. & Shah, V.B. (2015). Julia: A Fresh Approach to Numerical
370 Computing.

371 Blanchet, F.G., Cazelles, K. & Gravel, D. (2020). Co-occurrence is not evidence of ecological interactions.
372 *Ecology Letters*, 23, 1050–1063.

373 Blaom, A.D., Kiraly, F., Lienart, T., Simillides, Y., Arenas, D. & Vollmer, S.J. (2020). MLJ: A Julia package
374 for composable machine learning. *Journal of Open Source Software*, 5, 2704.

375 Boakes, E.H., Rout, T.M. & Collen, B. (2015). Inferring species extinction: The use of sighting records.
376 *Methods in Ecology and Evolution*, 6, 678–687.

377 Canard, E., Mouquet, N., Marescot, L., Gaston, K.J., Gravel, D. & Mouillot, D. (2012). Emergence of
378 Structural Patterns in Neutral Trophic Networks. *PLOS ONE*, 7, e38295.

379 CaraDonna, P.J., Petry, W.K., Brennan, R.M., Cunningham, J.L., Bronstein, J.L., Waser, N.M., *et al.* (2017).
380 Interaction rewiring and the rapid turnover of plantpollinator networks. *Ecology Letters*, 20, 385–394.

381 Carlson, C.J., Dallas, T.A., Alexander, L.W., Phelan, A.L. & Phillips, A.J. (2020). What would it take to
382 describe the global diversity of parasites? *Proceedings of the Royal Society B: Biological Sciences*, 287,
383 20201841.

384 Cazelles, K., Araújo, M.B., Mouquet, N. & Gravel, D. (2016). A theory for species co-occurrence in
385 interaction networks. *Theoretical Ecology*, 9, 39–48.

386 Closs, G.P. & Lake, P.S. (1994). Spatial and Temporal Variation in the Structure of an Intermittent-Stream
387 Food Web. *Ecological Monographs*, 64, 1–21.

388 de Aguiar, M.A.M., Newman, E.A., Pires, M.M., Yeakel, J.D., Boettiger, C., Burkle, L.A., *et al.* (2019).
389 Revealing biases in the sampling of ecological interaction networks. *PeerJ*, 7, e7566.

390 Gauzens, B., Legendre, S., Lazzaro, X. & Lacroix, G. (2013). Food-web aggregation, methodological and
391 functional issues. *Oikos*, 122, 1606–1615.

392 Giacomuzzo, E. & Jordán, F. (2021). Food web aggregation: Effects on key positions. *Oikos*, 130,
393 2170–2181.

394 Griffiths, D. (1998). Sampling effort, regression method, and the shape and slope of sizeabundance

relations. *Journal of Animal Ecology*, 67, 795–804.

Gupta, A., Figueroa H., D., O’Gorman, E., Jones, I., Woodward, G. & Petchey, O.L. (2023). How many predator guts are required to predict trophic interactions? *Food Webs*, 34, e00269.

Hadfield, J.D., Krasnov, B.R., Poulin, R. & Nakagawa, S. (2014). A Tale of Two Phylogenies: Comparative Analyses of Ecological Interactions. *The American Naturalist*, 183, 174–187.

Havens, K. (1992). Scale and Structure in Natural Food Webs. *Science*, 257, 1107–1109.

Johnson, E.K. & Larremore, D.B. (2021). Bayesian estimation of population size and overlap from random subsamples.

Jordano, P. (2016). Sampling networks of ecological interactions. *Functional Ecology*, 30, 1883–1893.

Joseph, M.B. (2020). Neural hierarchical models of ecological populations. *Ecology Letters*, 23, 734–747.

Kenall, A., Harold, S. & Foote, C. (2014). An open future for ecological and evolutionary data? *BMC Evolutionary Biology*, 14, 66.

Khoshraftar, S. & An, A. (2022). A Survey on Graph Representation Learning Methods.

Koleff, P., Gaston, K.J. & Lennon, J.J. (2003). Measuring beta diversity for presenceabsence data. *Journal of Animal Ecology*, 72, 367–382.

Kopelke, J.-P., Nyman, T., Cazelles, K., Gravel, D., Vissault, S. & Roslin, T. (2017). Food-web structure of willow-galling sawflies and their natural enemies across Europe. *Ecology*, 98, 1730–1730.

Li, M., Liu, R.-R., Lü, L., Hu, M.-B., Xu, S. & Zhang, Y.-C. (2021). Percolation on complex networks: Theory and application. *Physics Reports*, Percolation on complex networks: Theory and application, 907, 1–68.

MacDonald, A.A.M., Banville, F. & Poisot, T. (2020). Revisiting the Links-Species Scaling Relationship in Food Webs. *Patterns*, 1.

Makiola, A., Compson, Z.G., Baird, D.J., Barnes, M.A., Boerlijst, S.P., Bouchez, A., *et al.* (2020). Key Questions for Next-Generation Biomonitoring. *Frontiers in Environmental Science*, 7.

Martinez, N.D., Hawkins, B.A., Dawah, H.A. & Feifarek, B.P. (1999). Effects of Sampling Effort on Characterization of Food-Web Structure. *Ecology*, 80, 1044–1055.

421 McLeod, A., Leroux, S.J., Gravel, D., Chu, C., Cirtwill, A.R., Fortin, M.-J., *et al.* (2021). Sampling and
 422 asymptotic network properties of spatial multi-trophic networks. *Oikos*, 130, 2250–2259.

423 Moore, A.L. & McCarthy, M.A. (2016). Optimizing ecological survey effort over space and time. *Methods*
 424 *in Ecology and Evolution*, 7, 891–899.

425 Niedballa, J., Wilting, A., Sollmann, R., Hofer, H. & Courtiol, A. (2019). Assessing analytical methods for
 426 detecting spatiotemporal interactions between species from camera trapping data. *Remote Sensing in*
 427 *Ecology and Conservation*, 5, 272–285.

428 Paine, R.T. (1988). Road Maps of Interactions or Grist for Theoretical Development? *Ecology*, 69,
 429 1648–1654.

430 Poisot, T. (2022). Guidelines for the prediction of species interactions through binary classification.

431 Poisot, T., Bergeron, G., Cazelles, K., Dallas, T., Gravel, D., MacDonald, A., *et al.* (2021). Global knowledge
 432 gaps in species interaction networks data. *Journal of Biogeography*, 48, 1552–1563.

433 Poisot, T., Ouellet, M.-A., Mollentze, N., Farrell, M.J., Becker, D.J., Brierly, L., *et al.* (2022). Network
 434 embedding unveils the hidden interactions in the mammalian virome.

435 Poisot, T., Stouffer, D.B. & Gravel, D. (2015). Beyond species: Why ecological interaction networks vary
 436 through space and time. *Oikos*, 124, 243–251.

437 Ponisio, L.C., Gaiarsa, M.P. & Kremen, C. (2017). Opportunistic attachment assembles plantpollinator
 438 networks. *Ecology Letters*, 20, 1261–1272.

439 Savage, V.M., Gillooly, J.F., Brown, J.H., West, G.B. & Charnov, E.L. (2004). Effects of Body Size and
 440 Temperature on Population Growth. *The American Naturalist*, 163, 429–441.

441 Song, C., Simmons, B.I., Fortin, M.-J. & Gonzalez, A. (2022a). Generalism drives abundance: A
 442 computational causal discovery approach. *PLOS Computational Biology*, 18, e1010302.

443 Song, C., Simmons, B.I., Fortin, M.-J., Gonzalez, A., Kaiser-Bunbury, C.N. & Saavedra, S. (2022b). Rapid
 444 monitoring for ecological persistence.

445 Stephenson, P. (2020). Technological advances in biodiversity monitoring: Applicability, opportunities
 446 and challenges. *Current Opinion in Environmental Sustainability*, Open issue 2020 part A: Technology
 447 Innovations and Environmental Sustainability in the Anthropocene, 45, 36–41.

448 Stock, M., Poisot, T., Waegeman, W. & De Baets, B. (2017). Linear filtering reveals false negatives in
 449 species interaction data. *Scientific Reports*, 7, 45908.

450 Strydom, T., Catchen, M.D., Banville, F., Caron, D., Dansereau, G., Desjardins-Proulx, P., *et al.* (2021). A
 451 roadmap towards predicting species interaction networks (across space and time). *Philosophical*
 452 *Transactions of the Royal Society B: Biological Sciences*, 376, 20210063.

453 Thompson, P.L. & Gonzalez, A. (2017). Dispersal governs the reorganization of ecological networks under
 454 environmental change. *Nature Ecology & Evolution*, 1, 1–8.

455 Thompson, R.M. & Townsend, C.R. (2000). Is resolution the solution?: The effect of taxonomic resolution
 456 on the calculated properties of three stream food webs. *Freshwater Biology*, 44, 413–422.

457 Volkov, I., Banavar, J.R., Hubbell, S.P. & Maritan, A. (2003). Neutral theory and relative species abundance
 458 in ecology. *Nature*, 424, 1035–1037.

459 Walther, B.A., Cotgreave, P., Price, R.D., Gregory, R.D. & Clayton, D.H. (1995). Sampling Effort and
 460 Parasite Species Richness. *Parasitology Today*, 11, 306–310.

461 Williams, R.J. & Martinez, N.D. (2000). Simple rules yield complex food webs. *Nature*, 404, 180–183.

462 Willott, S.j. (2001). Species accumulation curves and the measure of sampling effort. *Journal of Applied*
 463 *Ecology*, 38, 484–486.

464 Young, J.-G., Valdovinos, F.S. & Newman, M.E.J. (2021). Reconstruction of plantpollinator networks from
 465 observational data. *Nature Communications*, 12, 3911.

466 Zhang, S., Tong, H., Xu, J. & Maciejewski, R. (2019). Graph convolutional networks: A comprehensive
 467 review. *Computational Social Networks*, 6, 11.